View metadata, citation and similar papers at core.ac.uk

brought to you by CORE

provided by ANSTO Publications Online

Journal of Applied Physics

Low energy photoelectron diffraction analysis at high angular resolution of Cu and Mn/Cu surfaces

Cite as: J. Appl. Phys. **106**, 093510 (2009); https://doi.org/10.1063/1.3253329
Submitted: 09 July 2009 . Accepted: 21 September 2009 . Published Online: 09 November 2009

G. P. Cousland, A. E. Smith, J. D. Riley, and A. P. J. Stampfl

View Online

Export Citation

ARTICLES YOU MAY BE INTERESTED IN

New display-type analyzer for the energy and the angular distribution of charged particles
Review of Scientific Instruments **59**, 545 (1988); https://doi.org/10.1063/1.1139884

Wide-angle display-type retarding field analyzer with high energy and angular resolutions
Review of Scientific Instruments **88**, 123106 (2017); https://doi.org/10.1063/1.4990769

Time- and angle-resolved photoemission spectroscopy of solids in the extreme ultraviolet at 500 kHz repetition rate
Review of Scientific Instruments **90**, 023104 (2019); https://doi.org/10.1063/1.5081938

Lock-in Amplifiers up to 600 MHz

Watch

AIP Publishing

© 2009 American Institute of Physics.

Low energy photoelectron diffraction analysis at high angular resolution of Cu and Mn/Cu surfaces

G. P. Cousland,[1] A. E. Smith,[1,a)] J. D. Riley,[2] and A. P. J. Stampfl[3]
[1]*School of Physics, Monash University, Clayton, Victoria 3800, Australia*
[2]*Department of Physics, La Trobe University, Bundoora, Victoria 3086, Australia*
[3]*Bragg Institute, Australian Nuclear Science and Technology Organisation, Lucas Heights, New South Wales 2234, Australia and School of Chemistry, The University of Sydney, New South Wales 2006, Australia*

(Received 9 July 2009; accepted 21 September 2009; published online 9 November 2009)

X-ray photoelectron diffraction simulations using a real-space approach are shown to accurately produce the extraordinarily detailed photoelectron diffraction pattern from Cu{111} at an electron kinetic energy of 523.5 eV. These same simulations show that most sensitivity is obtained when using low energy electrons at high angular resolution. Structural differences are observed to be greatest around a kinetic energy of ~100 eV and many of the features observed in the photoelectron diffraction patterns may be directly related to phenomena observed in low energy electron diffraction patterns from the same surface. For Cu{100}, simulations of buckled surfaces with a Mn overlayer predict that low energy photoelectron diffraction can easily discriminate chemical and structural differences. Even the effects of the relaxed surface of Cu{100} is indeed observable along azimuthal scans around a kinetic energy of 100 eV. Our results show that low energy photoelectron diffraction is extremely sensitive to changes in surface structure if high resolution patterns are acquired. © *2009 American Institute of Physics*. [doi:10.1063/1.3253329]

I. INTRODUCTION

X-ray photoelectron diffraction (XPD) is an established experimental technique used for the determination of surface structure.[1,2] One of the strengths of XPD is that it uses specific core levels and is therefore atom specific enabling diffraction patterns from adsorbates and particular components of alloys.[3,4] If chemical shifts are large enough atoms with particular bonding can be selected as electron sources.

Typical XPD energies in the range of 200–1000 eV are used in which regime multiple scattering significantly contributes to the electron intensity distribution as does forward scattering. In its earliest incarnation, much structural information was obtained with diffraction patterns at energies above 300 eV from forward focusing and Kikuchi-like effects,[5,6] for data along the lines of atoms.[7] More recently simulations and *R* factor analysis have provided a means of comparing data with complex structures and enabling atomic positions to be determined with reasonable accuracy. Single scattering models were widely used but as multiple scattering analyses appeared it became clear that single scattering models did not yield correct interatomic spacing.

Two developments have offered an improvement for XPD determination of surface structures. Electron diffraction in atomic clusters (EDAC) software[8] has enabled the calculation of multiple scattering processes for large clusters and can simulate XPD patterns with a higher degree of resolution. Electron analyzers have improved resolution enabling data to be obtained with more detailed angular structures being resolved and data taken over the full 2π steradians. In this paper we compare the EDAC calculation of the diffraction patterns from a Cu(111) surface and the experimental data set to show detailed comparison which is now possible.

This paper explores the sensitivity of full hemisphere photoelectron diffraction to variations in the bulk terminated structure of Cu(100) surfaces and to a bulk terminated structure with a Mn overlayer. It is noted that most low energy electron diffraction (LEED) determination of surface structures is performed at low electron energies so the examination of sensitivities ranges from electron energies in the usual range, 300 eV down to typical LEED energies of 50 eV. Comparison is made between the bulk terminated diffraction pattern and the varied surfaces using an *R* factor whose values give an objective determination of the changes in the diffraction data and the possibility of structure determination from full hemispherical photoelectron diffraction (FHPED).

Comparison is shown between the experimental diffraction pattern from a Cu(111) surface for $3p$ electrons with an energy of 523 eV and the calculated diffraction pattern using EDAC code. The remarkable agreement suggests that using EDAC to explore the sensitivity of FHPED as a function of energy for different surface structures will guide and demonstrate its value for surface determination.

The present work has been prompted by an investigation of the exchange properties at the interface of antiferromagnetic and ferromagnetic materials with spin glass surfaces. Cu_3Mn has been chosen as the initial material, with azimuth-scanned synchrotron XPD patterns to be used to determine structure. In the present work, owing to the growth properties of the CuMn alloy,[9] XPD diffraction patterns for Cu {100} surfaces are considered in comparison with Mn/Cu{100} using low photoelectron energies. Due to the enhanced ability of current electron spectrometers, XPD can now be obtained at higher angular resolution than has previously been the case. While only preliminary experimental results are available,[10] computer simulations are carried out using EDAC

a)Electronic mail: andrew.smith@sci.monash.edu.au.

 © 2009 American Institute of Physics

to determine how well low energy photoelectron diffraction analysis can find structure. These simulations are thus predictions of high resolution XPD results in the energy range below ~300 eV.

As the variation with energy of the reflected intensity is an integral part of LEED surface analysis,[11] XPD patterns may depend strongly on low kinetic energies. Accordingly Cu{100} XPD patterns at values in the range 73.5–303.5 eV for bulk truncated, relaxed,[12] buckled, and Mn incorporated surfaces[9] are investigated using EDAC. An *R*-factor analysis is used to compare data from the bulk truncated Cu{100} simulation with the other Cu surfaces simulated, for all energies investigated.

In order to check the accuracy of the simulations for copper surfaces, EDAC calculations are carried out for the Cu{111} surface as experimental results for this surface are now available from a second generation toroidal electron spectrometer, which is able to achieve high angular resolution.[13] While comparisons of EDAC simulations with experimental results for Cu{111} have been made previously,[14] the present work shows how performing a high resolution analysis enables the observation of an extraordinary amount of detail in a XPD pattern of Cu{111}.

II. SIMULATION REQUIREMENTS

EDAC simulates XPD and LEED by summing in real space over scattering paths, with atoms represented by muffin tin potentials,[15] arranged in clusters. Results were calculated with the modified recursion method, which is an extension of Haydock's method.[16] Diffraction patterns were determined for hemispherical 2π scans over all polar and azimuthal angles at fixed energies. Simulations were performed for a parabolic cluster, with the emitting atom positioned at the focus of the solid paraboloid.

The simulation time scales with the product $nN^2(l_{\max}+1)^3$ where n is the number of iterations, N the number of atoms in the cluster, and $l_{\max}$ the maximum angular momentum quantum number for the scattering event, estimated from the photoelectron energy.[15] N depends on energy through the corresponding volume, proportional to the cube of the inelastic mean free path, which is energy dependent.[17] For convergence to be achieved at high resolution, the number of iterations required was typically greater than 40. Together with required cluster sizes of approximately 1300 atoms, this was substantially greater than the literature values.[8]

Separate simulations were run for emitters on different atomic planes and the output added together in order to construct a diffraction pattern. These simulations could thus be run concurrently on separate processors in a high performance computing environment. The composite data were then displayed as a stereographic projection of an XPD pattern.

III. *R*-FACTOR ANALYSIS

To examine simulation data quantitatively, a modified *R*-factor formulation is used to compare the bulk truncated Cu{100} with the relaxed, buckled, and Mn incorporated surfaces. The *R*-factor is found by first calculating a χ value that is the (normalized) difference between the intensity at a point $I(\theta,\phi)$ and the averaged azimuthal intensity over the corresponding polar angle $I(\theta)$, for each data set,[18]

$$\chi(\vartheta,\phi) = [I(\vartheta,\phi) - I_0(\vartheta)]/I_0(\vartheta). \quad (1)$$

Following Zheng *et al.*,[19] the *R*-factor was then determined as the sum of squares of the difference of the χ values between two data sets employing an appropriate normalization,

$$R = \frac{\Sigma_i(\chi_{ci} - \chi_{ei})^2}{\Sigma_i(\chi_{ci}^2 + \chi_{ei}^2)}, \quad (2)$$

where χ_{ci} are the simulated and χ_{ei} the experimental (including background subtraction) χ values. For comparison purposes in the present work the bulk truncated Cu{100} simulation was taken as the "experimental" χ values.

IV. CU{111} AT (3*P*) ELECTRON KINETIC ENERGY OF 523.5 EV

An experimental diffraction pattern for Cu{111} was acquired at an electron kinetic energy of 523.5 eV using a toroidal electron spectrometer designed and built by the Centre for Materials and Surface Science (CMSS) at the La Trobe University, Department of Physics, and now installed and operational at the Berlin synchrotron facility BESSY.[13] The spectrometer allows the *simultaneous* analysis of a range of kinetic energies of emitted electrons at all polar angles. This approach dramatically reduces measurement time in comparison to a conventional angle resolved photoelectron spectrometer, which measures photoelectrons for one combination of polar and azimuthal angles at a time. The CMSS spectrometer allows for the rotation of the sample for obtaining data at different azimuth angles. By combining a set of polar scans taken at different azimuth angles, a full hemisphere scan can be constructed. Importantly the toroidal design and parallel nature of acquisition allows the full angular resolution of the analyzer to be used without increasing data acquisition times unduly. Typically three dimensional diffraction patterns taken from single crystal Cu surfaces take less than 30 min to acquire.

Figure 1 shows symmetrized experimental and EDAC simulated diffraction patterns for Cu{111} at an electron kinetic energy of 523.5 eV from a Cu 3*p* core level. All diffraction patterns shown are contrast images, where low and high intensity features are shown as dark and light regions, respectively. As the resolution of the toroidal analyzer is 0.5° and 1° in the polar and azimuthal angles, respectively, the angular resolution for both the azimuthal and polar angles in the EDAC simulations was set to 0.5° and accordingly allows the testing of features found in the experiment at this resolution.

The results shown in Fig. 1, at a photoelectron kinetic energy of 523.5 eV, may be compared with lower resolution results obtained for Cu{111} using the 2*p* core level excited with Mg $K\alpha$ and Si $K\alpha$ at electron kinetic energies of $E_{\text{kin}}=320.8$ eV and $E_{\text{kin}}=807.2$ eV, respectively.[14] These experimental results were successfully simulated by EDAC, with the main features attributed to forward focusing and Kikuchi-like bands.

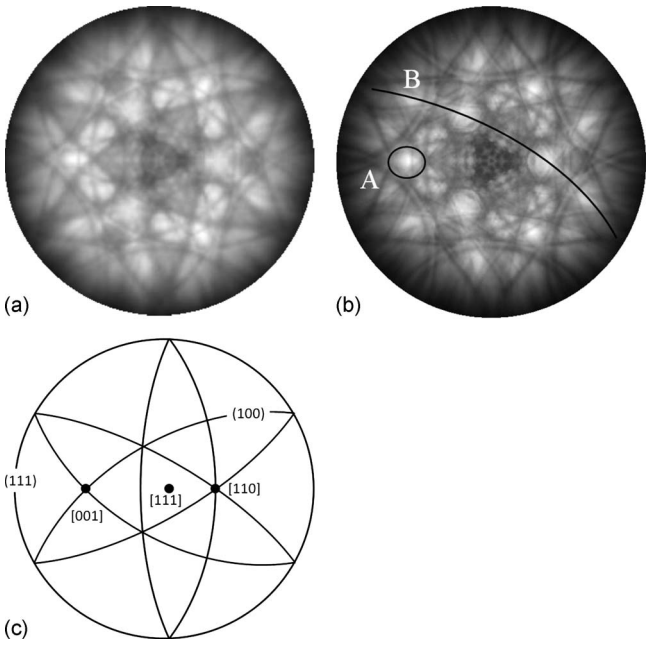

FIG. 1. Comparison between experimental XPD patterns for Cu{111} with a photoelectron kinetic energy of 523.5 eV and stereographically projected EDAC simulations. (a) Experimental (b) simulation with photoelectron emitted from the 3*p* shell at a kinetic energy of 523.5 eV at 300 K; (c) the planar and axial projections for Cu{111}. Label A marks forward focusing along the [001] principal axes and label B Kikuchi bands.

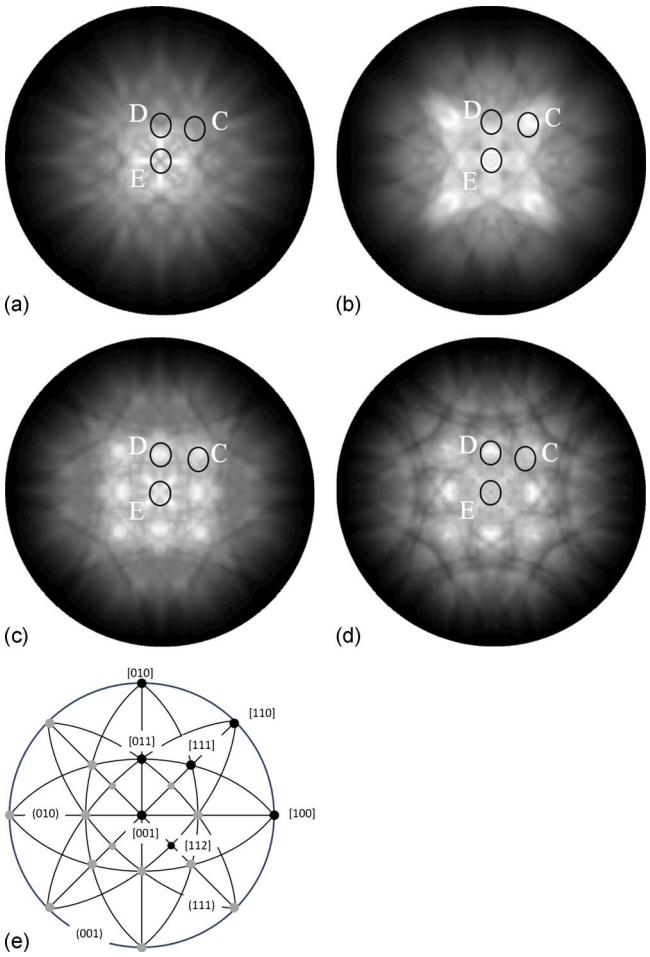

FIG. 2. (Color online) Stereographic projection of EDAC output at temperature of 300 K for electron kinetic energies (a) 73.5 eV, (b) 103.5 eV, (c) 203.5 eV, and (d) 303.5 eV. (e) is the stereographic projection for bulk truncated Cu{100}. Label C marks the [111] principal axis, D [011], E [001]. The images demonstrate forward focusing and Kikuchi-like bands at photoelectron energies of 103.5 eV and above. Note the minimum in the [001] center (e) of the diffraction pattern at a photoelectron energy of 73.5 eV.

It should be emphasized that in order to reproduce the high resolution of the present calculation compared with the earlier work, larger clusters and a higher number of iterations are required for the calculations to converge. In particular the present calculation uses 44 iterations and cluster sizes of ~2700 atoms, which is approximately ten times greater than that of the earlier work. These findings for Cu{111} show that EDAC clearly replicates the XPD experimental result at high resolution, including forward focusing (labeled "A" in figure) and Kikuchi bands (B).

V. CU{100} IN (3*P*) ELECTRON KINETIC ENERGY RANGE OF 73.5–303.5 EV

Figure 2 shows the results of XPD simulations from bulk truncated Cu{100} at 300 K performed for electron kinetic energies of 73.5, 103.5, 203.5, and 303.5 eV. The results are displayed in Fig. 2 as contrast images of Cu{100} diffraction patterns at 300 K, where photoelectrons are emitted from 3*p* core levels. In these simulations the sample is moved through polar and azimuthal angles, with an angle of 55° being maintained between source and detector that are in the same plane. This configuration corresponds to XPD synchrotron experiments performed using a SPECS 150 MCD electron spectrometer at the National Synchrotron Radiation Research Centre, Taiwan. In this series of measurements the detector was set to an angular resolution of 1° in both polar and azimuthal directions, which were defined by a five axis manipulator from OmniVac.

Forward focusing can be expected at energies above ~300 eV for XPD patterns,[5] but Fig. 2 predicts this at lower energies. While not evident at 73.5 eV, the 103.5 eV XPD pattern shows forward focusing along the [111] principal axes (label "C" in Fig. 2) as does the 203.5 eV pattern along the [011] axes (label D). At 103.5 eV there is forward focusing in the center of the pattern along the [001] principal axis (label E) but this does not occur at 73.5 eV. As in LEED experiments for Cu{100},[11] these real-space simulations pre-

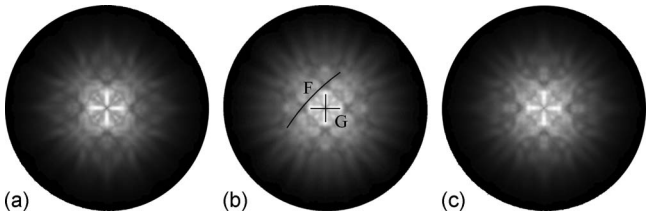

FIG. 3. Stereographic projection of (a) Cu{100} with surface relaxation of −1.10% for first, +1.70% second, +1.0% third interlayer spacing, (b) Cu{100} with an 0.5 ML Mn overlayer that is buckled, and (c) Cu{100} with the same buckle as in (b) for electron kinetic energy of 73.5 eV and at a temperature of 300 K. Bulk truncated Cu{100} is displayed in Fig. 2. Features in (b) include Kikuchi-like bands (f) that make the central white cross (g) appear smaller. The parameters for surface relaxation in (a) come from Davis and Noonan (Ref. 12) and the buckle in (b) and (c) comes from Wuttig *et al.* (Ref. 9). *R* factors comparing data from these results with Fig. 2(a) are shown in Table I.

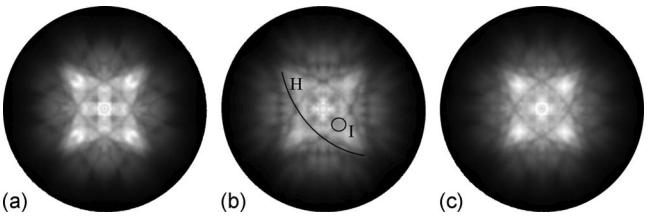

FIG. 4. Simulated diffraction patterns with electron kinetic energy of 103.5 eV. Other parameters as in Fig. 3. Extra features in (b) include stronger Kikuchi patterns (h) and four intensity minima associated with [112] axes (i).

dict that XPD patterns are energy dependent. For instance XPD simulations show an overall drop in intensity at higher energies as seen in LEED. It is also possible to identify XPD features with LEED intensity variations. For example, the central minimum for the [001] axis at 73.5 eV corresponds to the minimum of intensity in the 00 beam for LEED at ~73 eV.[11]

Figures 3–6 show results of EDAC calculations for electrons emitted from Cu 3*p* levels and *various* Cu{100} based structures for kinetic energies of 73.5, 103.5, 203.5, and 303.5 eV. Each figure compares three surfaces: (a) relaxed Cu{100},[12] (b) buckled Cu{100} with Mn overlayer,[9] and (c) the same buckled Cu{100} with only Cu atoms. Bulk truncated Cu{100} at the corresponding energies is displayed in Fig. 2.

Results of *R*-factor calculations are displayed in Table I. They show comparisons between the results displayed in Fig. 2 with those of Figs. 3–6 using a scheme based on Eqs. (1) and (2). Overall the diffraction patterns for Cu{100} with surface relaxation closely resemble those for bulk truncated Cu{100} at all energies shown. As seen in Table I, this can be further verified by the low *R* factors.

Considering results at a kinetic energy of 73.5 eV, Fig. 3(b) shows that Cu{100} with a buckle and Mn overlayer is especially distinguished by dark lines corresponding to sections of {111} Kikuchi-like bands (labeled "F" in figure) that surround the central region. The *R* factor is 0.26, the highest value obtained (see Table I). These bands make the central white cross (label G) in Fig. 3(b) appear smaller than in the other XPD patterns of Fig. 3. At a kinetic energy of 103.5 eV Fig. 4(b) shows that the pattern for buckled Cu{100} with Mn overlayer might appear most distinct, but the *R*-factor value of 0.21 is in fact slightly smaller than for the buckled only

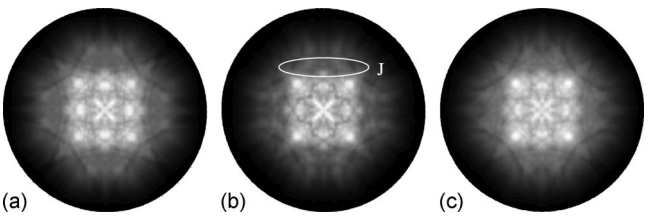

FIG. 5. Contrast images with electron kinetic energy of 203.5 eV. Other parameters as in Fig. 3. Although variation between patterns is more subtle than at lower energies, differences can still be observed. The comparison of relaxed (a) and buckled (c) Cu{100} simulations indicates significant similarity, and Cu{100} with an Mn overlayer (b) exhibits some extra features, including less distinct Kikuchi bands (j) and a less intense (darker) outer region.

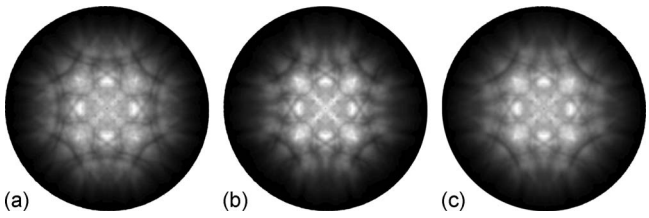

FIG. 6. Contrast images at an electron kinetic energy of 303.5 eV. Other parameters as in Fig. 3. No obvious differences are observed for the patterns shown at this energy.

Cu atoms (*R* factor of 0.22). In particular the {111} Kikuchi patterns (label "H") together with four intensity minima that can be associated with [112] axes (label I) appear more clearly in Fig. 4(b).

Finally, the visual differences between diffraction patterns at 203.5 and 303.5 eV (Figs. 5 and 6, respectively) for relaxed and bulk truncated surfaces as well as for the Mn/Cu systems investigated here are quite subtle and show that higher energy patterns are less sensitive to fine changes in surface structure. At 203.5 eV, the Mn/Cu pattern shows some small differences, such as less distinct Kikuchi lines (label "J" in Fig. 5) and generally lower intensity outside the central region of the pattern. Any distinction at 303.5 eV is difficult to discriminate, with little visible evidence of difference in the patterns for the various structures. The *R* factors at 303.5 eV (see Table I) also indicate this, with values of 0.0012 for the relaxed surface of Davis and Noonan[12] and 0.0031 for the surface due to Fowler and Barth.[20] At 303.5 eV the *R* factor of 0.24 for Cu with a Mn overlayer is close to the value of 0.20 for the buckled Cu surface.

While overall the diffraction patterns for Cu{100} with surface relaxation closely resemble those for bulk truncated Cu{100} at all energies shown, and also evidenced by the *R* factors given in Table I, interestingly, however, low energy azimuthal diffraction scans show quite large differences between the currently different proposed relaxation models of

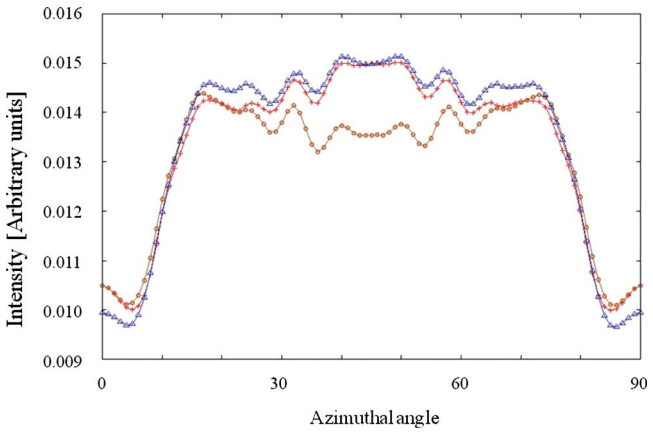

FIG. 7. (Color online) Comparison of Cu 3*p* intensities for azimuthal scans at polar angle of 30° for Cu{100} at 300 K and electron kinetic energy of 103.5 eV. Surface relaxation parameters from (+) Davis and Noonan, Δd_{12} −1.10%, Δd_{23}+1.70%, Δd_{34}+1.0% (Ref. 12), (○) Fowler and Barth, Δd_{12} −2.0%, Δd_{23}+1.0% (Ref. 20), (△) without surface relaxation. The intensity scale is linear. Note that at 0° and 90° the 3*p* intensities for relaxed surfaces coalesce, whereas at 45° the intensity of the surface from Fowler and Barth exhibits difference.

TABLE I. *R*-factor comparisons between simulated values of bulk truncated Cu{100} with the simulated data for (a) Cu{100} with surface relaxation parameters from Davis and Noonan (Ref. 12) and (b) with surface relaxation of −2.0% first, 1.0% second interlayer spacing from Fowler and Barth (Ref. 20), (c) Cu{100} with a Mn overlayer that is buckled, and (d) Cu{100} with the same buckle as in (c). See Fig. 3 for details of structural parameters.

Kinetic energy (eV)	Relaxed Cu{100}, Davis and Noonan	Relaxed Cu{100}, Fowler and Barth	Cu{100} with buckle and Mn overlayer	Cu{100} with buckle
73.5	0.0041	0.0061	0.26	0.16
103.5	0.0015	0.0054	0.21	0.22
203.5	0.0042	0.0068	0.17	0.14
303.5	0.0012	0.0031	0.24	0.20

Cu{100}. Comparison between these[12,20] show differences as great as 20%–30% of the total maximum intensity variation within a particular azimuthal scan, see Fig. 7. This is further evidenced by the *R* factors at 103.5 eV of 0.0015 for Davis and Noonan[12] surface relaxed Cu{100}[20] and 0.0054 for the surface due to Fowler and Barth.[20] Although small, these differences may be quantified by further *R*-factor analysis[21,22] or compared visually for particular scans as indicated by Fig. 7. These effects may be more evident at particular energies and so this method may use photoelectrons at kinetic energies optimized according to the surface being considered. Low energy photoelectron diffraction may be more sensitive than LEED in this regard as azimuthal distributions yield a plethora of information not attainable by LEED angular patterns from well ordered single crystalline surfaces.

VI. CONCLUSION

We have demonstrated how EDAC can be run at high resolution to successfully simulate highly detailed XPD patterns for the Cu{111} surface. In addition we have shown how EDAC predicts visible changes in Cu{100} XPD patterns as a function of energy and how working in a low kinetic energy regime may be used to determine structure. Low energy XPD has features in common with LEED, including an overall drop in intensity at higher energies and strong variations in intensity for the individual diffraction features. We have predicted that surface relaxation has little visible effect compared to bulk truncated Cu{100} for photoelectron energies of 73.5 and 103.5 eV as has been found in LEED. Unlike conventional LEED, however, there are some conditions in *k*-*E* space from low energy photoelectron diffraction that do indeed show significant differences between competing models in the low kinetic energy regime. This was evidenced in Cu{100} surfaces with small relaxation parameter differences by both *R*-factor analysis of full data sets and visual comparison of an azimuthal scan. Thus low energy photoelectron diffraction may be more sensitive than LEED in determining small changes to surface structure because of the effect of multiple scattering from core-level electrons that yields incredibly detailed diffraction patterns. *R*-factor analysis used to compare bulk truncated Cu{100} with the other cases indicates a noticeable effect caused by introducing buckles and an Mn overlayer at all energies simulated. Although visible similarity would indicate that there is little difference in diffraction patterns at 303.5 eV, *R*-factor analysis indicates differences in intensities comparable to those of patterns at lower energies investigated. Finally we conclude that high resolution XPD simulations for Cu{100} at 300 K can visibly discriminate element types and buckles in surfaces, at kinetic energies below 303.5 eV, compared to the bulk truncated case, and that having performed high resolution experiments, a combination of data sets *R* factor analysis and visual analysis will provide a method to accurately distinguish structural models.

ACKNOWLEDGMENTS

G.C. would like to thank Dr. Steve Homolya for running the original Cu{111} simulation and providing shell scripts and many helpful ideas about operating EDAC. The simulations were run at the Victorian Partnership for Advanced Computing.

[1] D. P. Woodruff, J. Electron Spectrosc. Relat. Phenom. **126**, 55 (2002).
[2] C. S. Fadley, in *Synchrotron Radiation Research: Advances in Surface and Interface Science*, edited by R. Z. Bachrach (Plenum, New York, 1992), Vol. 1, p. 421.
[3] C. Westphal, Surf. Sci. Rep. **50**, 1 (2003).
[4] J. Osterwalder, P. Aebi, R. Fasel, D. Naumovic, P. Schwaller, T. Kreutz, L. Schlapbach, T. Abukawa, and S. Kono, Surf. Sci. **331–333**, 1002 (1995).
[5] W. F. Egelhoff, Jr., Crit. Rev. Solid State Mater. Sci. **16**, 213 (1990).
[6] D. Naumovic, A. Stuck, T. Greber, J. Osterwalder, and L. Schlapbach, Phys. Rev. B **47**, 7462 (1993).
[7] M.-L. Xu, J. J. Barton, and M. A. Van Hove, Phys. Rev. B **39**, 8275 (1989).
[8] F. J. Garcia de Abajo, M. A. Van Hove, and C. S. Fadley, Phys. Rev. B **63**, 075404 (2001).
[9] M. Wuttig, C. C. Knight, T. Flores, and Y. Gauthier, Surf. Sci. **292**, 189 (1993).
[10] G. P. Cousland, A. E. Smith, J. Riley, S. Homolya, A. Stampfl, and J. King-Lacroix, Proceedings of the 32nd Condensed Matter and Materials Meeting, 29 January−1 February 2008, Wagga Wagga. Available from: http://www.aip.org.au/wagga2008/.
[11] J. B. Pendry, J. Phys. C **4**, 2514 (1971).
[12] H. L. Davis and J. R. Noonan, J. Vac. Sci. Technol. **20**, 842 (1982).
[13] L. Broekman, A. Tadich, E. Huwald, J. Riley, R. Leckey, T. Seyller, K. Emtsev, and L. Ley, J. Electron Spectrosc. Relat. Phenom. **144–147**, 1001 (2005).
[14] L. Despont, D. Naumovic, F. Clerc, C. Koitzsch, M. G. Garnier, F. J. Garcia de Abajo, M. A. Van Hove, and P. Aebi, Surf. Sci. **600**, 380 (2006).
[15] J. B. Pendry, *Low Energy Electron Diffraction* (Academic, London, 1974).
[16] R. Haydock, Solid State Phys. **35**, 215 (1980).
[17] C. J. Powell and A. Jablonski, J. Phys. Chem. Ref. Data **28**, 19 (1999).

[18]R. Fasel, P. Aebi, J. Osterwalder, L. Schlapbach, R. G. Agostino, and G. Chiarello, Phys. Rev. B **50**, 14516 (1994).
[19]J.-C. Zheng, C. H. A. Huan, A. T. S. Wee, M. A. Van Hove, C. S. Fadley, F. J. Shi, E. Rotenberg, S. R. Barman, J. J. Paggel, K. Horn, Ph. Ebert, and K. Urban, Phys. Rev. B **69**, 134107 (2004).
[20]D. E. Fowler and J. V. Barth, Phys. Rev. B **52**, 2117 (1995).
[21]E. Zanazzi and F. Jona, Surf. Sci. **62**, 61 (1977).
[22]J. B. Pendry, J. Phys. C **13**, 937 (1980).